

PETROLOGY AND GEOCHEMISTRY OF JANCHIVLAN GRANITE PLUTON, CENTRAL MONGOLIA

O. GEREL¹, S. KANISAWA², K. ISHIKAWA³, SH. HIZUMI⁴, S. AMAR-AMGALAN¹ and
S. JARGALAN³

¹Dept. of geology & Mineralogy, Mongolian University of Science and Technology, P.O. 46, Box 520,
Ulaanbaatar. E-mail: gerel@mtu.edu.mn

²Dept. of Earth and Environmental Science, Faculty of Science, Yamagata University, Yamagata 990-
8560, Institute of Mineralogy, Japan;

³Institute of Mineralogy, Petrology and Economic Geology, Tohoku University, Sendai 980-8578, Japan,

⁴Department of Geology, Shimane University, Matsue 690, Japan.

Abstract

Janchivlan pluton is a composite body comprising three distinctive phases intruded into late Paleozoic turbidites in the internal part of the Mongol-Okhotsk foldbelt. Granites are peraluminous and strongly peraluminous, felsic, with elevated alkalinity, high Fe/Mg ratio and low CaO, rich in K, Rb, Ta, Li and Sn. The content of these elements increased during fractional crystallization from first phase porphyritic coarse-grained granites through two mica granites of second phase and to Li-F granites of the third phase. Trace elements discrimination diagram is indicative of within-plate tectonic setting, but also display syn-collisional signature for first and second phases. Initial ⁸⁷Sr/⁸⁶Sr ratio is 0.7049-0.7044 for first and second phases accordingly, and 0.7187-0.7306 for third phase granites and 0.7502 for albite-lepidolite granites, indicating that source magma derived from the continental crust. Amazonite-albite granites show very high initial Sr ratio characterizing role of metasomatic processes in their origin. Granites are interpreted as having formed after collision in an intracontinental environment and are close to A2 type after Eby. These are originated from continental crust, but high K content characteristic for all phases show important role of deep source. Miagritic pegmatites, Sn, W greisens and veins, alluvial Sn and Ta, Li mineralization is associated with these granites.

Introduction

Mesozoic granitic magmatism occurs in the Khentey uplift of Central Mongolia. The Khentey uplift is a part of extent, the 1000 km wide, Mongol-Okhotsk fold belt stretched from Khangai mountain in Central Mongolia up to the Pacific Ocean over 3000 km. (Zonenshain et al., 1976). Two main stages of Mesozoic magmatic events are distinguished: Early Mesozoic (170-240 Ma) and Late Mesozoic (100-170 Ma) based on mainly K-Ar and very few Pb-U and Rb-Sr dating. (Kovalenko et al., 1994; Koval, 1998). In Mesozoic in a large territory of Central and Eastern Mongolia the continental crust has been formed and Mesozoic magmatism developed in the mature continental crust. (Geology of Mongolia, 1973; Tectonics of Mongolia, 1974). Mesozoic intrusive episodes were interpreted as an tectonic and magmatic activation (Nagibina, 1967; Shtseglov, 1968), continent-continent collision (Zonenshain et al., 1990), plume activity (Koval, 1998).

Granitoids occupy about 150 sq.km (Koval, 1988). Mesozoic intrusive magmatism characterized by quartz diorite-granodiorite-granite or bimodal gabbro-granite series and shallow high-evolved granitic intrusions in the most internal part of the Mongol-Okhotsk fold belt. These granites have been described as rare metal granites with Li-F facies. (Kovalenko et al., 1971). High interest to Li-F granites is for their economic source of rare metals: Sn, W, Ta and Li. Magmatic genesis of Li-F granites proposed by Kovalenko et al. (1971); and experimentally studied by Kovalenko and Kovalenko. (1976). Based on geological mapping at scale 1:50000 and geochemical study rare metal granites were interpreted as a typical S-type, but with A-type granite features. (Gerel, 1990).

Janchivlan pluton of high-evolved granites was chosen as an example of granites with a potential rare metal (Sn, Li, Ta and Nb) mineralization. This paper presents a new isotopic and geochemical data that have made a contribution to understand genesis of high-evolved granites.

Regional Geology

The regional geology of the Khentei uplift consists of Vendian-early Cambrian, early Paleozoic-Carboniferous turbidites and volcanic rocks intruded by late Paleozoic-Mesozoic granitoids. Mesozoic granitoids occupy about 50% of the Khentei Uplift. It consists of more than 160, mostly metaluminous subalkalic to weakly alkalic intermediate to felsic intrusions that form simple to multiphase complexes. (Koval, 1998). Individual intrusions range from homogenous to zoned and include batholiths plutons and dikes. Granodiorites and granites are the main rock types. Minor phases include gabbro and diorites. Late pegmatites and aplites are very common. Locally late phases of batholiths have a slightly peraluminous composition that reflects late-stage fractionation. (Koval et al., 1984; Gerel, 1990). Internal part of the plutonic belt is occupied by small shallow intrusions of calc-alkaline series of elevated alkalinity and end members of Li-F granites. Intrusions are unfoliated crosscut the country rocks and are surrounded by contact-metamorphic aureoles of hornfels or have tectonic contact.

Volcanic rocks coeval with the intrusions have not been identified.

The regional structure is characterized by strike-slip faults that disply dominant northeast trends and east-west trends.

Geologic setting of Janchivlan pluton

Janchivlan pluton (Fig. 1A) is located 70 km southeast of Ulaanbaatar city on the southern spurs of the Khentei Range (southern part of the Paleozoic Khentei uplift). It was studied in detail by Kovalenko et al. (1971), Ivanov et al., 1984; Gerel (1990).

Host rocks consist of Precambrian metamorphic quartz-chlorite-sericite schists with quartzite lenses, the Middle Paleozoic sandstones and siltstones, intruded by Late Paleozoic granodiorites and plagiogranites. The main trend of Paleozoic structures is northeastern, conformable with the Khentei synclinorium strike.

The Janchivlan pluton is composed of high-evolved granites of Early Mesozoic age (K-Ar age 188-231 Ma and Rb-Sr age 190±2.1 Ma). The area occupied by Janchivlan pluton is 1100 sq.km. Pluton shows a complicate form with its apex directed to northeast a major direction of Mesozoic fault system.

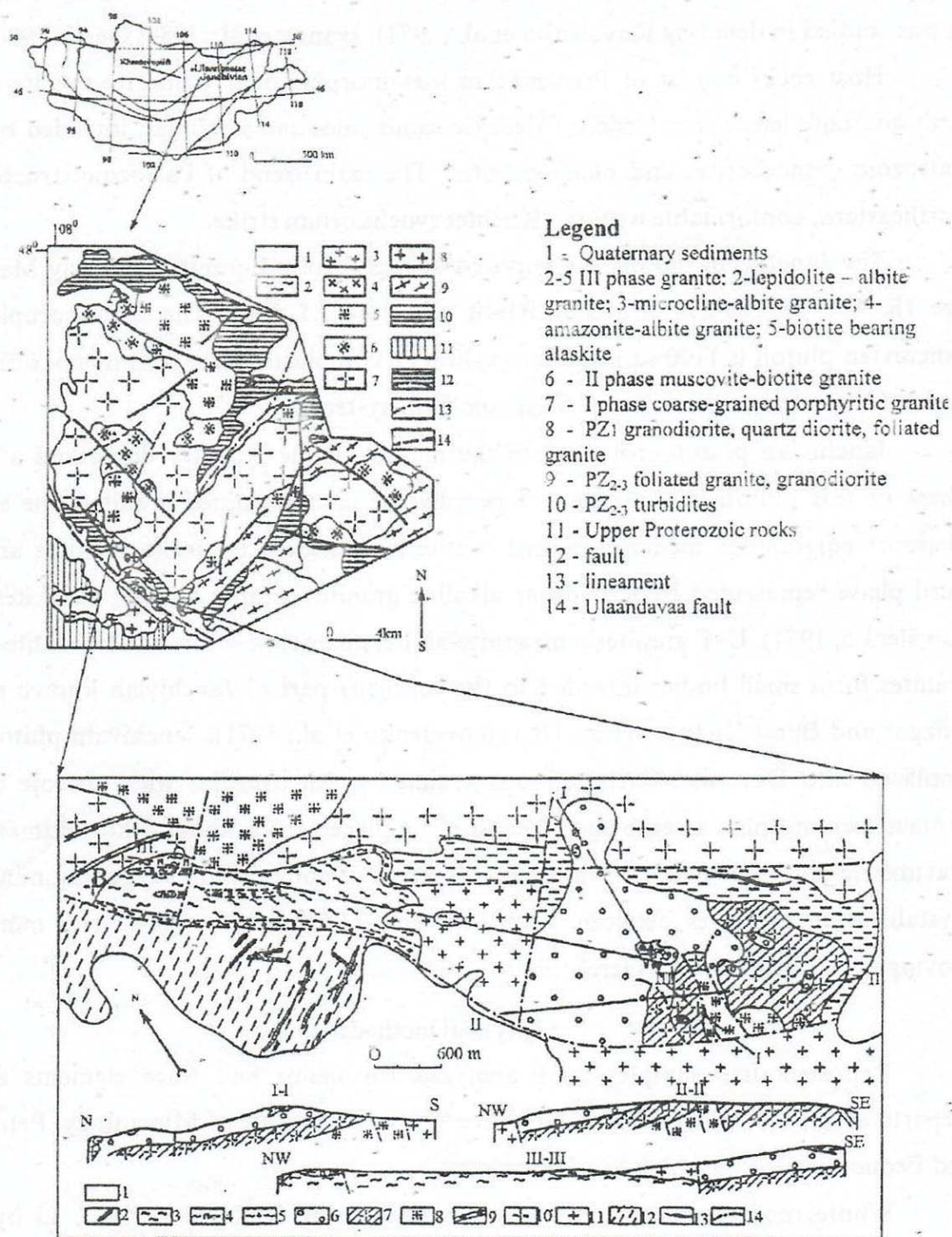
Janchivlan pluton crops out in the margin of the Khentey dome and a major phase of this pluton is composed of porphyritic coarse-grained granites, the second phase of eqigranular medium-grained biotite and muscovite-biotite granites and the third phase represented by K-feldspar alkaline granites (biotite bearing alaskites after Kovalenko, 1971). Li-F granites: amazonite-albite, microcline-albite and lepidolite-albite granites form small bodies intruded to the southern part of Janchivlan known as Urt Gozgor and Bural Khangai (Fig. 1B) (Kovalenko et al., 1971). Janchivlan pluton was emplaced into Devonian-Carboniferous sediments. An irregular wide aureole exhibits contact metamorphic assemblages. Depth of emplacement is about 7 km estimated by gravimetric data. (Novoselov et al., 1984) Normative composition suggesting minimum crystallization pressures between 1 and 0.5 kbar (Luth et al., 1964) with minimum moving to Ab enrichment. (Gerel, 1990)

Analytical methods

Representative samples were analyzed for major and trace elements at the Department of Geoscience, Shimane University and Institute of Mineralogy, Petrology and Economic Geology, Tohoku University.

Whole rock chemical analyses were made using RIX -2000 XRF, Li by ion-electrode method and Rb by atomic absorption spectrophotometry.

Extraction of Rb, Sr, from whole rock and mineral powders were carried out in a glass 1000 clean room at the Department of Geoscience, Shimane University, following



1 - Quaternary sediments, 2 - dikes of pegmatite and quartz veins, 3 - lepidolite-albite granite; 4 - lepidolite-albite pegmatitic granite; 5 - fine-grained albite-lepidolite granite; 6 - amazonite-albite granite; microcline-albite granite; 7 - biotite-bearing alaskite; 8 - I phase granite dikes, 10 - I phase porphyritic granite; 11 - PZ granodiorite and quartz diorite; 12 - PZ_{2,3} turbidites; 13 - diabase dike, 14 - fault

Fig. 1. (A) Geological simplified map of Janchivlan pluton (after Kovalenko et al., 1971). (B) Geological simplified map of Buural Khnagai and Urt Gozgor area with Li-F granites (after Kovalenko et al., 1971)

the method described by Iizumi (1996). $^{87}\text{Sr}/^{86}\text{Sr}$ ratio were normalized to $^{86}\text{Sr}/^{88}\text{Sr}=0.1194$

Mica was analyzed by combination of conventional gravimetry, the ion-electrode method (F) and atomic absorption spectrophotometry (Na_2O , K_2O , Li_2O and Rb_2O and electron probe microanalyser.

Petrography

Granites are high evolved and display high silica trend (72%-77%) SiO_2 from porphyritic coarse grained biotite granite to Li mica-albite granites. (Kovalenko et al., 1971; Ivanov et al., 1984; Gerel, 1990).

First phase porphyritic coarse-grained biotite granite occupied about 65% of intrusion area. It contains K- feldspar $\text{Or}_{75}\text{Ab}_{25}$ as phenocrysts and in groundmass $\text{Or}_{86}\text{Ab}_{14}$ (45-65%), quartz (30-35%), plagioclase An_{24-26} (10-15%) and biotite (3-5%), allanite, apatite, zircon, magnetite and ilmenite as accessory minerals and chlorite as secondary mineral. Coarse-grained biotite granites became equigranular biotitic and leucocratic and contain a number of miarolitic pegmatites.

Second phase granites occupy about 25% of intrusion area and are represented by medium grained weakly porphyritic biotite granite composed of K- feldspar $\text{Or}_{75}\text{Ab}_{25}$ (40-45%), plagioclase (10-15%), quartz (32-25%), biotite (4-6%) and muscovite (2%) and accessory minerals are allanite, apatite, zircon and magnetite

Third phase biotite-bearing leucogranites (alaskites) occupy about 17% of pluton area and Li-F granites (microcline-albite and amazonite-albite) about 6% and lepidolite-albite granites 1% accordingly. They composed of K-feldspar (36-38%), plagioclase An_{15-5} (15-23%), quartz (38-40%), biotite (3-4%) and accessory minerals: topaz, fluorite, monazite, columbite, ilmenite, and magnetite. Biotite bearing leucogranites crop out in the northeastern part of the pluton and form the Ulaanburd stock. They are associated with microcline-albite and amazonite albite granites in the southwestern part of the pluton in Buural Khangai outcrop (Fig.1B). Latter and the Urt Gozgor outcrop of rare metal granites have asymmetric dome shape elongated in the northwestern direction. They belonging to large Ulaan Davaa fault and are fractured into key like blocks by northeastern faults, plumaged the Ulaan Davaa fault.

The Buural Khangai outcrop (Fig.1A) has a concentric zonal structure. Microcline-albite granites are light yellow medium grained rocks composed of dark gray quartz (40%), perthitic K-feldspar (30.5%), albite An_{7-10} , sometimes sugar like albite An_{2-4}

(25.5%) and accessory mica: protolithionite and light Li fengite. Other accessory minerals are topaz, fluorite, zircon, monazite, columbite, xenotime, cassiterite and magnetite.

Amazonite-albite granites are light colored, medium grained, poorly porphyritic composed of light gray quartz (38-39%), blue green amazonite (35%), white albite (21%) and accessory minerals (protolithionite-zinnwaldite) and topaz, fluorite, zircon, monazite, columbite and cassiterite.

Albite-lepidolite granites composed of quartz, K-feldspar (14%), albite (57%), lepidolite (4%) and topaz (2-2.5%). Some contain up to 10% topaz and up to 20 % lepidolite. . Albitites have up to 90 % of albite, 3% microcline, 3% quartz, 2.5% lepidolite and 0.4% topaz. Accessory minerals are fluorite, zircon, monazite, columbite, Pb-pyrochlore and cassiterite. There are massive chilled, moderate porphyritic, abundant-porphyritic and pegmatitic (Kovalenko et al., 1971). Contact between porphyritic granite and albite-lepidolite granites was checked by two-drill hole at the depth of 67-106 m. (Sizykh et al., 1984)

Albite, quartz, K-feldspar and Li-mica are the major rock-forming minerals. Magmatic topaz is common accessory mineral. Quartz is unihedral. Lepidolite is very abundant K feldspar is unihedral, poikilitic Quartz crystals are idiomorphic. Granite is greisenized and fluorite is common for all types of Li-F granites. Cassiterite is also common.

Mica forms trend from siderophyllite in first phase granites to lepidolite and zinnwaldite from third phase (Tab. 1.Fig.2, 3).

Lithium is one of the essential constituent elements in micas especially in the Li-F granites, pegmatites and greisen that associate with Nb and REE elements.

Tischendorf et al. (1997) proposed the estimation of Li_2O from the empirical relationships between Li_2O and SiO_2 , MgO , F and Rb in trioctahedral micas and between Li_2O and F as well as Rb in dioctahedral micas. After that they partially revised the equations between the relation of Li_2O and MgO in Li-micas due the difference in the tectonic environments of granites (Tischendorf et al., 1999).

We present the analytical data by means of the electron probe microanalysis of the other Li-bearing micas from Janchivlan and one analysis from amazonite granite of the Avdrant plutons. Most of the mica belong to the low Li-Mg group, therefore their Li_2O contents were calculated from the equation of $\text{Li}_2\text{O}=[0.9/(0.26 + \text{MgO})] - 0.05$ by Tischendorf et al. (1999). Some micas in J-5 and J-14 are rich in SiO_2 and low in

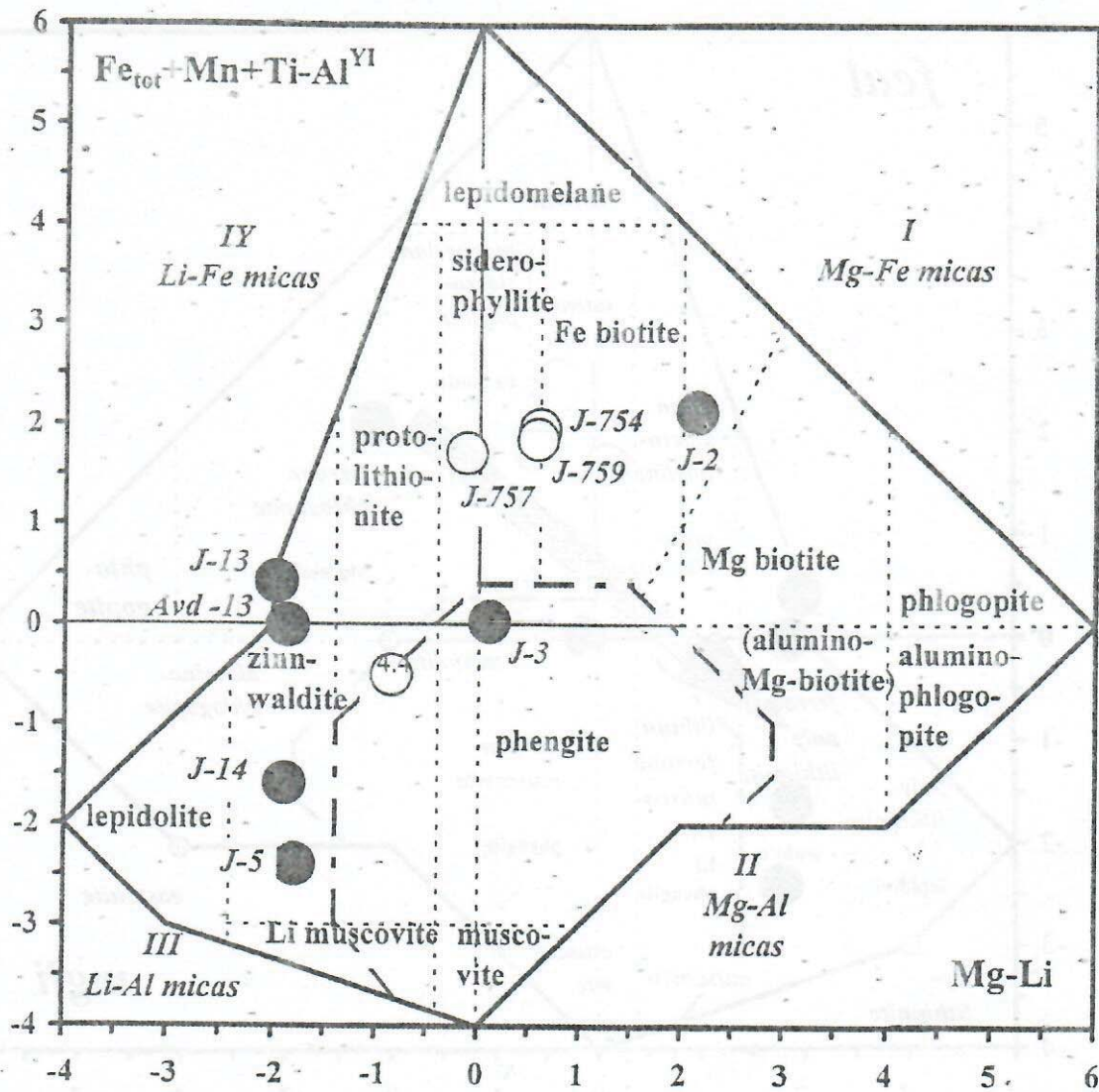


Fig.2. Micas from granites of Janchivlan pluton on the diagram of $[\text{Mg-Li}]$ vs. $[\text{Fe}_{\text{total}} + \text{Mn} + \text{Ti} + \text{Al}]$, with $R_{\text{VI}} = 4.4$ as the boundary between di- and trioctahedral micas (Tischendorf et al., 1997). J-754, J-757 and J-759 are biotites from I phase granites (Gerel unpublished data).

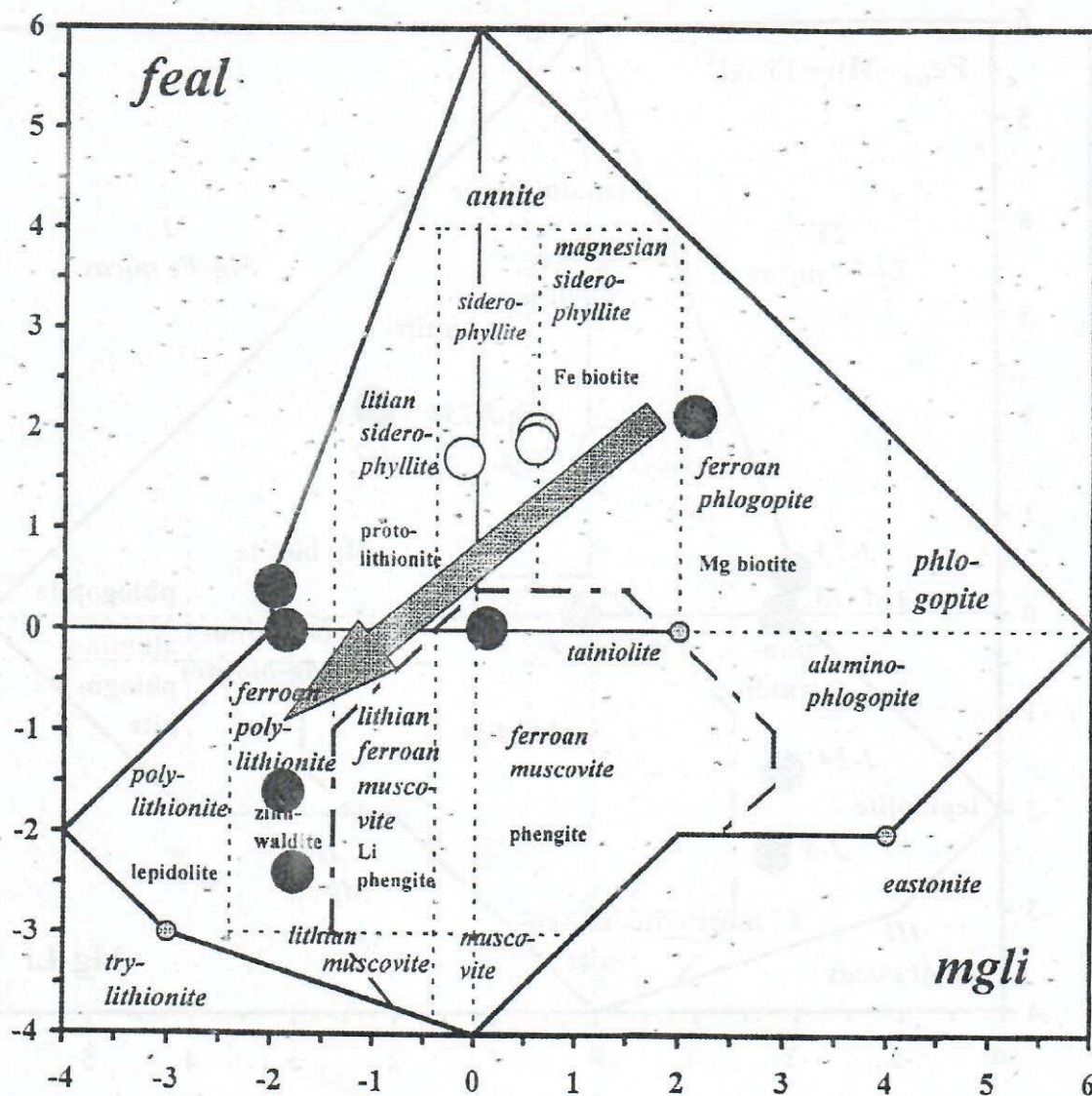


Fig.3. Trend of Li-F micas from Janchivlan plutons the diagram of Tischendorf et al. (1997) . IMA approved names are given in italics. *feal* = octahedral ($\text{Fe}_{\text{tot}} + \text{Mn} + \text{Ti} - \text{Al}^{\text{IV}}$); *mgli* = octahedral (Mg-Li).

Table 1. Average composition of microns from Janchuklan pluton

Sample No.	Avg-13	Ave-13 (n=13)		J-5 (n=10)		J-13 (n=13)		J-14 (n=10)		J-2 (n=6)		J-3 (n=3)	
P-Point No.	wet anal.	average	std dev.	average	std dev.	average	std dev.	average	std dev.	average	std dev.	average	std dev.
SiO ₂	43.47	44.48	0.76	56.56	2.22	41.05	3.25	54.01	2.35	37.13	0.50	38.43	2.30
TiO ₂	0.57	0.34	0.14	0.06	0.07	0.28	0.11	0.03	0.04	2.30	0.56	0.91	0.45
Al ₂ O ₃	21.49	21.44	0.36	19.69	1.16	22.68	0.72	17.85	1.12	16.50	1.25	18.92	1.33
Fe ₂ O ₃	6.01	-	-	-	-	-	-	-	-	-	-	-	-
FeO	9.27	14.15	0.64	2.00	1.38	17.95	3.45	3.97	1.43	19.06	0.66	24.03	3.87
MnO	0.17	0.33	0.04	0.59	0.39	0.44	0.10	2.89	0.91	0.55	0.03	0.57	0.02
ZnO	n.d.	0.76	0.06	0.06	0.12	0.31	0.08	0.15	0.11	n.d.	n.d.	n.d.	n.d.
MgO	0.03	-	-	0.01	0.01	-	-	-	-	9.49	0.27	0.54	0.03
Li ₂ O	3.24	3.41	0.00	3.31	0.16	3.36	0.11	3.38	0.09	0.04	0.00	1.08	0.04
CaO	0.03	0.00	0.01	0.02	0.02	-	0.01	0.01	0.01	0.01	0.01	0.00	0.00
Na ₂ O	0.36	0.25	0.05	0.19	0.08	0.15	0.08	0.09	0.04	0.14	0.03	0.17	0.02
K ₂ O	9.41	9.44	0.16	10.06	0.33	9.36	0.18	9.70	0.34	9.52	0.27	9.84	0.15
Rb ₂ O	0.91	0.30	0.09	0.49	0.10	0.30	0.09	0.61	0.13	n.d.	n.d.	n.d.	n.d.
H ₂ O ⁺ *	0.81	1.19	0.16	0.65	0.19	2.28	0.16	0.59	0.19	3.48	0.05	1.87	0.33
F	7.14	6.30	0.36	8.05	0.39	3.88	0.21	7.88	0.43	0.93	0.14	4.19	0.84
Total	102.91	102.42	0.54	102.02	0.48	102.04	0.48	101.17	0.62	99.15	0.29	100.55	0.38
O=F	3.01	2.65	0.15	3.63	0.16	1.64	0.09	3.32	0.18	0.39	0.06	1.76	0.35
Total	99.9	99.77	0.52	98.63	0.49	100.4	0.51	97.85	0.66	98.76	0.26	98.79	0.65

(O, OH, F=24)																		
Si	6.222	6.384	0.08	7.593	0.22	5.966	0.30	7.481	0.27	5.662	0.13	5.964	0.23					
Al(IV)	1.778	1.616	0.08	0.407	0.22	2.034	0.30	0.519	0.27	2.318	0.13	2.035	0.23					
Al(VI)	1.847	2.011	0.04	2.708	0.09	1.855	0.28	2.398	0.07	0.659	0.12	1.424	0.38					
Ti	0.061	0.037	0.02	0.005	0.01	0.031	0.01	0.003	0.00	0.265	0.06	0.108	0.05					
Fe ³⁺	0.647	-	-	-	-	-	-	-	-	-	-	-	-					
Fe ²⁺	1.110	1.698	0.08	0.226	0.16	2.195	0.46	0.462	-0.17	2.440	0.09	3.129	0.57					
Mn	0.021	0.040	0.00	0.079	0.05	0.054	0.01	0.339	0.11	0.071	0.00	0.075	0.00					
Zn	-	0.080	0.01	0.021	0.01	0.033	0.01	0.016	0.01	-	-	-	-					
Mg	0.006	-	-	0.002	-	-	-	-	-	2.165	0.06	0.124	0.01					
Li	1.865	1.969	0.01	1.788	0.07	1.968	0.10	1.885	0.05	0.026	0.00	0.675	0.02					
Ca	0.005	0.001	0.00	0.003	0.00	0.001	0.00	0.001	0.00	0.001	-	-	-					
Na	0.100	0.071	0.01	0.051	0.02	0.044	0.02	0.025	0.01	0.041	0.01	0.052	0.00					
K	1.718	1.729	0.03	1.723	0.06	1.738	0.05	1.715	0.06	1.859	0.05	1.950	0.02					
Rb	0.084	0.028	0.01	0.043	0.01	0.028	0.01	0.054	0.01	-	-	-	-					
F	3.232	2.856	0.16	3.415	0.17	1.788	0.11	3.450	0.17	0.448	0.05	2.053	0.38					
OH	0.769	1.144	0.16	0.595	0.17	2.212	0.11	0.550	0.17	3.552	0.06	1.947	0.38					
F+OH	4.000	4.000	-	4.000	-	4.000	-	4.000	-	4.000	-	4.000	-					

Y-site	5.557	5.835	0.06	4.823	0.13	6.138	0.3	5.103	0.18	5.626	0.09	5.535	0.24
tit or di	-	-	-	-	-	-	-	-	-	-	-	-	-
Al total	3.625	3.627	0.06	3.116	0.19	3.89	0.09	2.916	0.2	2.977	0.23	3.46	0.17

Mg-Li	-1.859	-1.968	0.01	-1.784	0.08	-1.968	0.1	-1.885	0.05	2.138	0.06	0.55	0.02
tit or di	-0.008	-0.238	0.12	-2.398	0.29	0.425	0.76	-1.594	0.28	2.129	0.16	1.987	1.00
Al total	-	-	-	-	-	-	-	-	-	-	-	-	-

H₂O⁺ are calculated as (F+OH) = 4.00 stoichiometry.

octahedral Y-site with $R^{(VI)} < 5.0$, therefore they may belong to the transitional type of tri- and di-octahedral micas. Tischendorf et al. (1999) recommended only micas with Y-site > 5.0 for the estimating Li_2O by correlation with MgO . Therefore, calculating the Li_2O of micas of J-5 and J-14 may have large errors. These micas may have more Li_2O concentration than calculated values. The concentration of H_2O also can not be determined, therefore the values were calculated as the stoichiometry of $(OH + F + Cl) = 4.00$. Some micas exceed 4.00 of the value $F + Cl$. Tischendorf et al. (1997) proposed the nomenclature of ideal micas from the position on a $Mg-Li$ vs. $Fe_{total} + Mn + Ti + Al^{(VI)}$ diagram. According to the diagram, the result of one wet analysis of Avd-12 by Tischendorf et al. (1999) is in good agreement with that of the conventional gravimetry. Mica in J-2 is rich in Fe and Mg, but poor in Li and belongs to Mg-biotite. Mica in J-3 is rich in Fe and poor in Mg, and contains about 1% of Li_2O , therefore it belongs to protolithionite. Mica in J-5 is rich in SiO_2 , F, and $Li_2O > 3\%$, but poor in Fe and Mg. Therefore it has Y-site cation less than 5, and belongs to zinnwaldite according the nomenclature of Tischendorf et al. (1997), however due to its low content in Y-site cation it is transitional between zinnwaldite and Li-muscovite. Micas in J-13 are rich in Fe, medium in Mg, Li and F, so belong to zinnwaldite. J-14 mica is medium in Fe, Mg, Li and F, therefore it belongs also to zinnwaldite.

The major trend of mica from granites of Janchivlan pluton (Fig. 3) is in a good agreement with mica analyzed by wet chemistry (Kovalenko et al., 1971; Lapidès et al., 1977)

Geochemistry

The chemical composition is shown in Table 2. Granites are silica rich (SiO_2 range from 72% to 78%, subalkaline, (Fig. 4A), peraluminous and strongly peraluminous (Fig.5). Major petrochemical characteristics of I and II phase granites are high silica content, elevated alkalinity, high Fe/Mg ratio, low CaO and high Al_2O_3 (Gerel, 1990). On Ab-Or-Q- H_2O diagram Li-F granites are plotted near the Ab corner. Granites are calc-alkaline and plot in the subalkaline field on TAS diagram. (Fig. 4A) and high K and shoshonitic field indicating elevated alkalinity. (Fig.4B). Granites are high evolved, but three phases are clearly recognized with maximum of 72% SiO_2 content for I phase, for second bimodal distribution with maximums in 70% and 74% SiO_2 and 75% SiO_2 for the third phase exhibit fractionation of silicic magma With increasing SiO_2 content Al_2O_3 ,

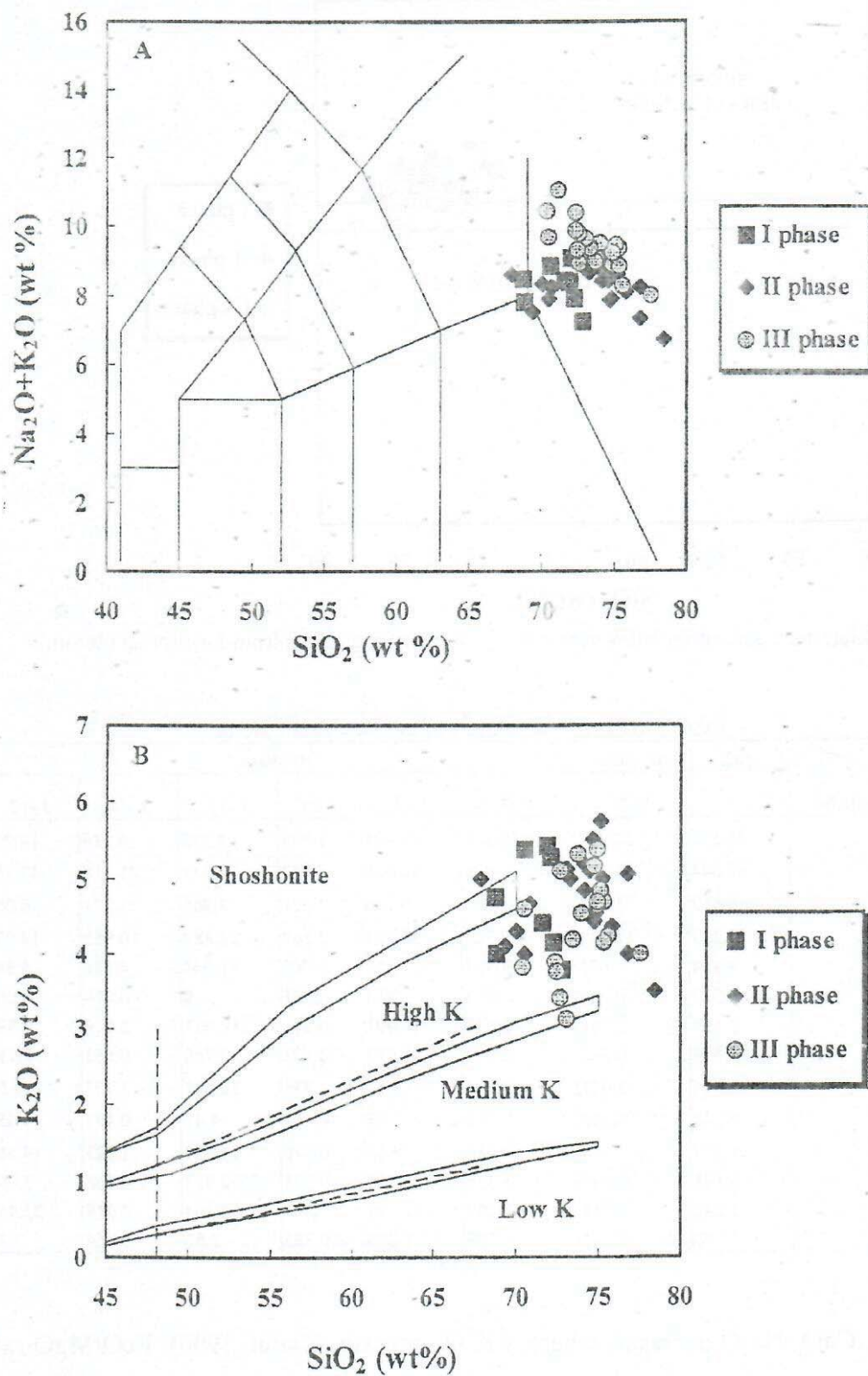


Fig. 4. Granites of Janchivlan pluton on the total alkalis-silica (TAS) diagram (A) and (B) on the K_2O - SiO_2 diagram (Le Maitre et al., 1989; Peccerillo and Taylor, 1976)

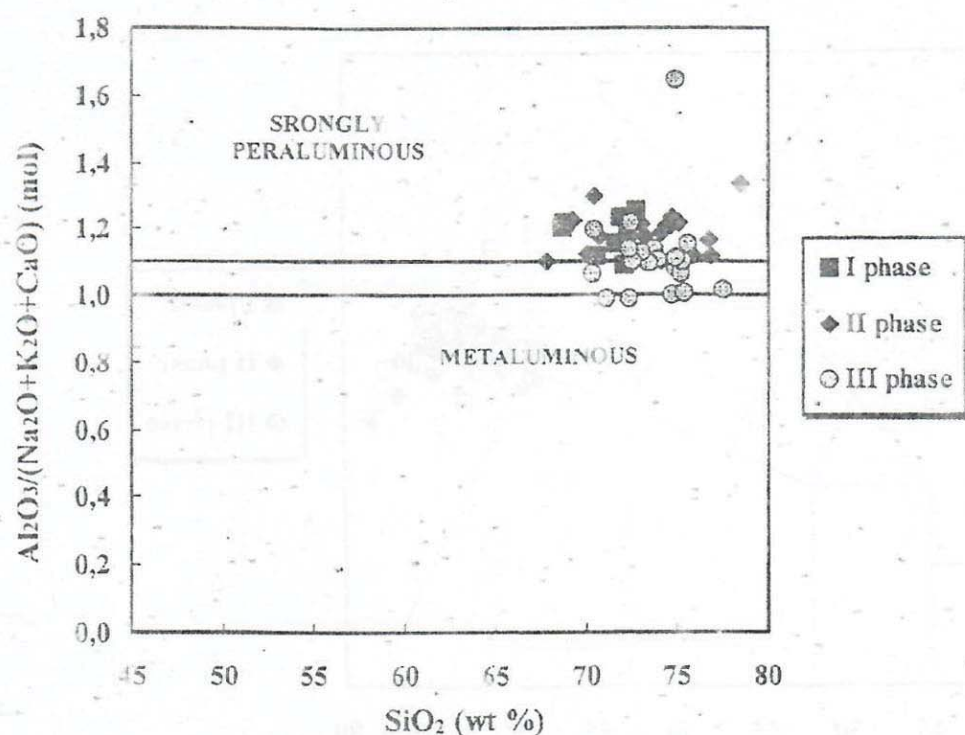


Fig.5. Aluminum saturation index versus silica content for granites from Janchivlan pluton.

Table 3. REE concentrations of the Janchivlan pluton

Elements	I phase	II phase	III phase					
Sample No	J-1	J-2	J-3	J-4	J-5	J-13	J-14	J-15
La	25.532	12.937	56.306	35.478	1.769	15.392	6.186	14.902
Ce	53.644	31.298	110.875	80.036	7.857	47.771	21.418	43.788
Pr	6.612	3.588	12.39	9.656	1.11	7.865	3.271	6.008
Nd	22.223	12.238	37.746	30.231	2.367	28.889	10.965	18.936
Sm	4.424	2.698	8.317	7.256	0.765	11.042	4.281	6.847
Eu	0.519	0.336	0.15	0.13	0.005	0	0.014	0.008
Gd	3.658	2.181	8.426	7.091	0.281	10.921	2.859	7.593
Tb	0.567	0.363	1.847	1.652	0.122	2.746	0.563	2.151
Dy	2.941	2.021	13.299	11.969	0.936	20.612	3.107	16.96
Ho	0.544	0.356	3.1	2.768	0.172	4.41	0.477	4.057
Er	1.339	0.936	9.985	9.33	0.676	14.494	1.325	14.569
Tm	0.195	0.147	1.825	1.794	0.228	2.917	0.262	3.093
Yb	1.242	0.918	12.207	12.791	2.425	20.334	1.919	23.468
Lu	0.173	0.131	1.708	1.803	0.335	2.82	0.264	3.46

TiO₂, MgO, CaO, Na₂O decrease, whereas K₂O increase. (Gerel, 1990). FeO/MgO ratio and K content are high. It seems to be a general characteristic of high-evolved granites.

There is distinct difference between granites represented I and II phases and III phase granites. High silica content, low CaO and MgO, high Fe/MgO ratio and elevated alkalinity characterize Li-F granites.

Trace element chemistry (Tab. 2) distinguishes I and II stage granites from the Li-F granites by low Ba, Sr and high Li, Nb, Rb, Y and Ga (Fig.6A). REE pattern (Tab. 3, Fig. 6B) show typical for evolved granites picture with high Eu anomaly.

In tectonic diagrams Rb vs. Y+Nb (Fig.7B) and Nb vs Y granites of Janchivlan pluton are plotted in the within plate granite field of Pearce et al. (1984) instead the I and II phases, which are plotted in the field of syn-collision or in the boundary between syn-collisional and within plate granite. (Gerel et al., 1999). Both I and II phases granites on the diagram $10000 \cdot \text{Ga}/\text{Al}$ vs. FeO^*/MgO and $10000 \cdot \text{Ga}/\text{Al}$ vs. $\text{Na}_2\text{O}+\text{K}_2\text{O}$ are plotted on the area close of I&S (mainly in the border). This is supported by diagram $1000 \cdot \text{Ga}/\text{Al}$ vs. Zr and SiO_2 vs. FeO^*/MgO where the I and II phase granites are plotted in the field of I & S in the border, but III phase granites outside of this field. On the diagram Y/Nb vs. Rb/Nb (Fig. 8A) they are plotted on the field A2 after Eby (1992). Trace element trends are generally as smooth as those of major elements: Rb, Ta, Nb, Th, increase, whereas Sr, Ti, Ba decrease from I to III phase compositions. Rare metal granites are enriched in Li, Be, Rb and F (Tab.2, Fig. 6A)

Mineralization

Every phase of granites is characterized by different mineralization. Miagrolitic pegmatites are associated with I stage porphyritic coarse grained biotite granites. Pegmatites have fine-grained and graphic texture, high Fe, SiO_2 and $\text{Na}_2\text{O}+\text{K}_2\text{O}$ content. They are belonged to miagrolitic mountain crystal-bearing pegmatites (Gerel, 1978; Ivanov et al., 1984). More than 200 pegmatite bodies are known. Rare metal pegmatites are associated with III phase granites. Sn-W mineralization is associated with II stage biotite-muscovite granites contained greisens and quartz veins with Sn, Sn-W and W mineralization and Sn placers. The most common are quartz-tourmaline, quartz-topaz and quartz-muscovite types. Zinwaldite-bearing greisen (zwitter) is also occurred in some area. (Kovalenko et al., 1971; Sizykh et al., 1984). Greisens are enriched in SiO_2 and depleted in alkalis, especially in Na. Albitites are depleted in silica and enriched in Na, sometimes up to 10.34% (Kovalenko et al., 1974). Urt Gozgor and Buural khangai

Table 2. Selected geochemical analysis of the Janchikhan pluton

Sample No	J-100	J-1	J-101	J-2	J-102	J-103	J-3	J-4	J-104	J-105	J-106	J-107	J-5	J-13	J-14	J-15
Major oxides (wt.%)	J-100	J-1	J-101	J-2	J-102	J-103	J-3	J-4	J-104	J-105	J-106	J-107	J-5	J-13	J-14	J-15
SiO ₂	73.93	70.6	76.25	72.44	75.9	75.97	76.56	77.23	72.77	77.3	76.03	74.46	68.76	75.07	73.85	77.61
TiO ₂	0.38	0.27	0.07	0.24	0.09	0	0.07	0.08	0	0.01	0	0	0	0.02	0.01	0.02
Al ₂ O ₃	13.86	15.11	13.14	14.46	12.87	14.29	12.26	12.5	17.34	13.59	14.87	16.84	18.16	13.88	14.84	11.92
Fe ₂ O ₃	1.25	0.57	0.53	0.13	0.68	0.25	0.24	0.24	0.17	0.28	0.08	0.1	0.12	0.13	0	0.21
FeO	1.16	1.4	0.67	1.33	0.7	0.39	0.87	0.93	0.08	0.31	0.09	0.06	0.13	0.58	0.39	0.63
MnO	0.06	0.05	0.03	0.06	0.04	0.02	0.03	0.03	0.17	0.02	0.05	0.15	0.07	0.02	0.15	0.02
MgO	0.51	0.32	0.15	0.63	0.13	0.11	0.03	0.04	0.13	0.13	0.13	0.11	0.03	0	0	0.01
CaO	1.39	0.91	0.54	1.21	0.61	0.29	0.4	0.38	0.64	0.27	0.19	0.24	0.41	0.2	0.08	0.12
Na ₂ O	3.45	3.61	3.76	3.55	3.83	4.54	3.7	3.88	5.63	4.79	3.73	5.59	6.37	5.03	5.22	3.45
K ₂ O	4.21	5.96	5.16	4.54	5.05	4.7	4.81	4.5	3.43	3.96	5.03	2.81	5.25	4.65	3.63	5.26
P ₂ O ₅	0.14	0.12	0	0.08	0.02	-	-	0.02	0	-	0	0.01	0	0.01	0.02	-
LOI	0.28	0.87	0.44	0.62	0.4	0.28	1.44	1.98	0.41	0.31	0.79	0.75	1.90	0.93	2.05	1.05
Total	100.6	99.79	100.72	99.29	100.32	100.85	100.41	101.81	100.77	100.97	100.99	101.13	100.98	100.52	100.24	100.3
Trace elements (ppm)																
Ba	285	500	111	303	196	68	91	97	200	63	204	191	230	-	-	-
Ce	128	-	162	-	197	85	-	-	36	73	17	3	-	-	-	8
Cr	16	-	13	18	10	7	-	-	11	6	12	19	3	-	6	34
Ga	22	21	39	20	36	54	28	29	66	53	67	74	58	38	40	-
Li*	-	135	-	148	-	-	248	400	-	-	-	-	2388	383	1681	743
Nb	16	15	45	11	42	26	39	46	48	38	26	34	116	30	50	85
Ni	25	3	27	5	29	28	8	5	33	28	32	33	16	7	7	9
Pb	19	25	32	44	33	94	30	54	60	78	34	57	29	81	46	100
Rb	205	285	664	238	657	744	626	719	2060	702	2149	1776	2311	842	2266	1408
Rb*	-	377	-	315	-	-	766	870	-	-	-	-	2887	707	2304	1397
Sr	118	127	14	108	28	2	11	11	17	1	9	18	10	-	6	0
Th	29	-	55	-	32	21	-	-	27	22	18	76	30	-	-	-
V	21	15	-	20	0	-	7	11	-	1	-	-	-	-	-	-
Y	42	30	148	14	138	171	131	113	264	145	262	223	59	188	114	142
Zr	186	165	140	105	137	67	169	155	35	67	9	19	31	79	42	164

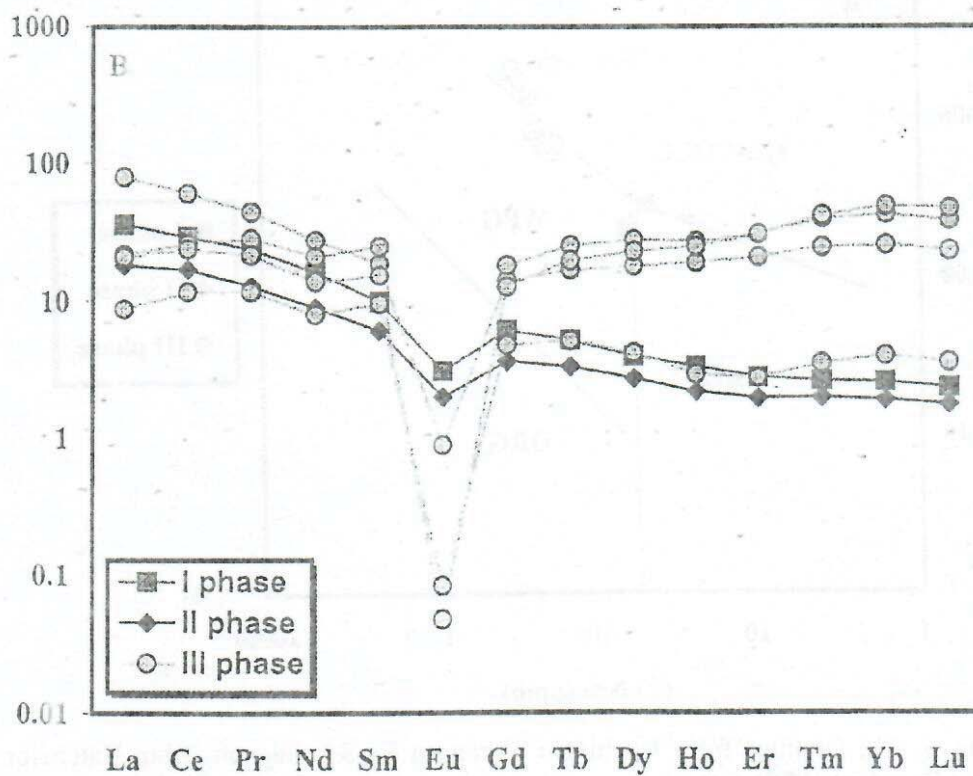
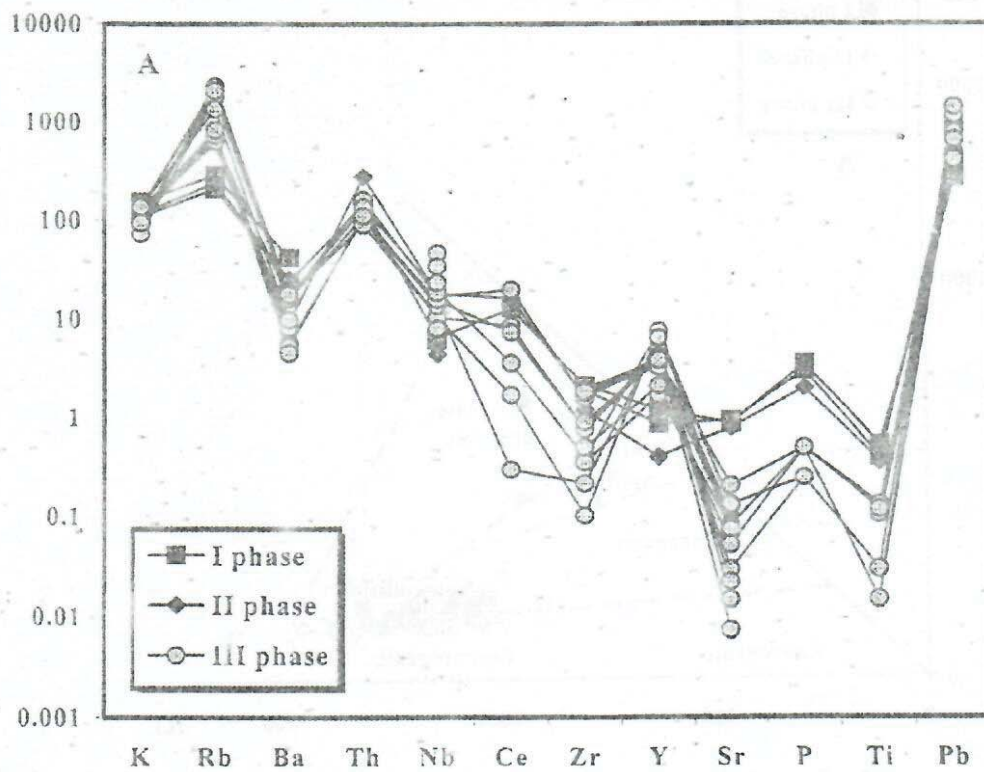


Fig. 6. (A) MORB normalized spiderdiagram for granites of Janchivlan pluton. (B) REE pattern for the Janchivlan pluton (normalized to primitive mantle, McDonough, 1992)

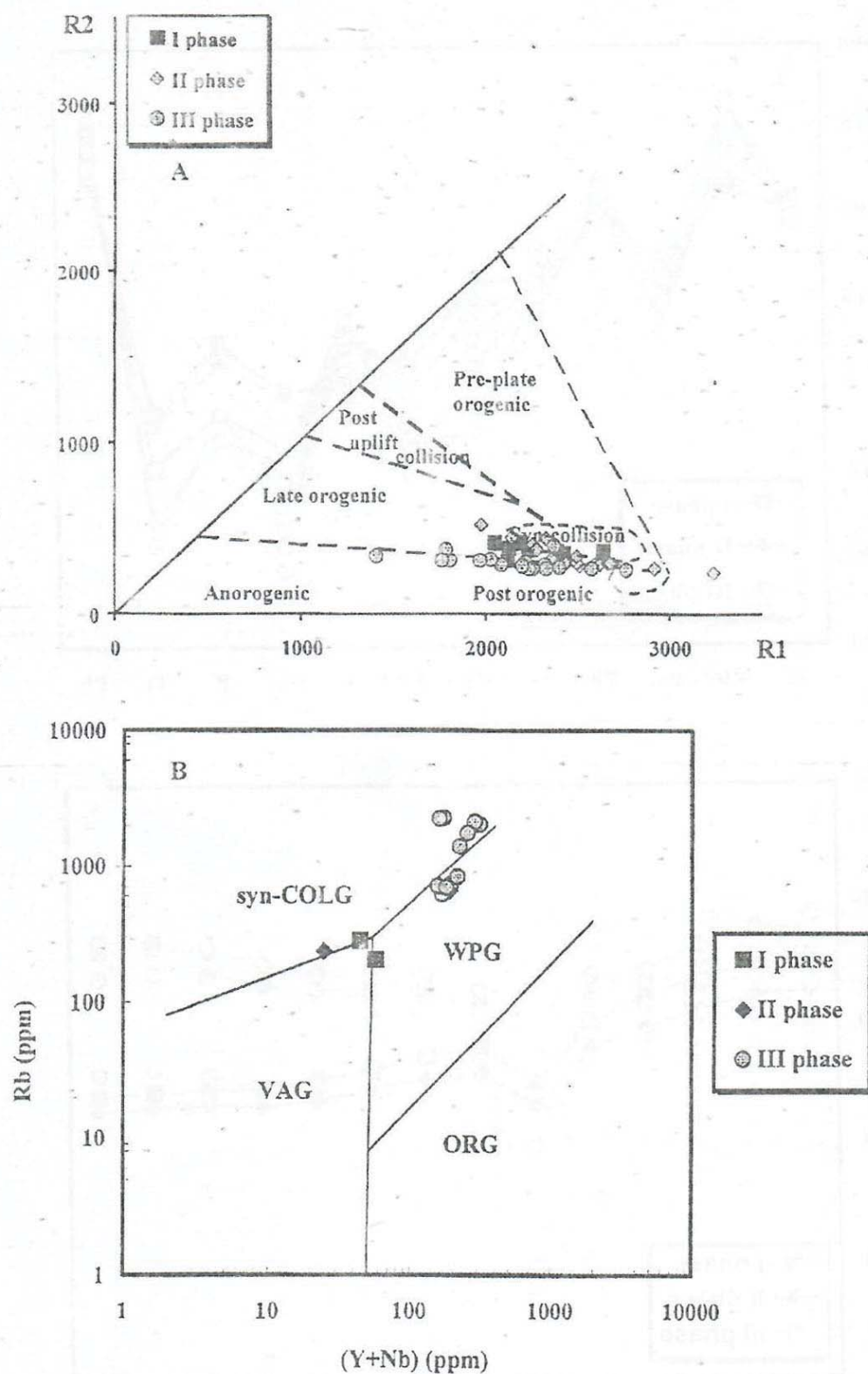


Fig. 7. (A) Granites from Janchivlan pluton on R1-R2 diagram (from Batchelor and Bowden, 1985). (B) Chemical composition of granites from Janchivlan pluton on the Rb versus (Y+Nb) discrimination diagram of Pearce et al., (1984)

(Fig.1B) with Ta, Li and albite-lepidolite granites of Urt Gozgor are the economic ore for Ta. Series of metasomatic rocks occur in Urt Gozgor area: lepidolite albitites, amazonitized albitites and quartz albitites (albite-lepidolite greizens (Kovalenko et al., 1971; Sizykh et al., 1984)..

Drill holes on the Urt Gozgor discovered the contact of albite-lepidolite granites with coarse-grained porphyritic granites of I phase on a depth of Albitites consists of albite (90%), microcline (3%); quartz (3%), lepidolite (2.5%) and topaz (0.4%). Granites from Janchivlan pluton are plotted on $\text{Fe}_2\text{O}_3/\text{FeO}$ vs. Rb/Sr diagram (Blewin et al., 1996) and show low oxidation state characteristic for Sn mineralization and fractionation of high evolved magma (Fig. 9A and B)

Discussion

Granites of the Janchivlan multiphase pluton were emplaced after continent-continent collision and closure of the Mongol-Okhotsk ocean resulting in voluminous granitic magmatism occurred as batholiths in the Khentei uplift's core and as shallow small plutons in interior of the Mongol-Okhotsk belt. On the R1-R2 diagram (7A) all granites, including data from Gerel, (1990), Koval, (1998) and new analyzed data are plotted in area of partly syn-collision and late and post-orogenic (Batchelor and Bowden, 1985) indicating within plate origin of granites. (Fig.7B; Fig. 8A). There is a significant increase in Nb, Y and Zr and a decrease in Ba and Sr from the I to III phase granite. The variation of these elements could be due the crystal fractionation, especially increases of Rb. Volatiles are considered to play an important role in the petrogenesis of Li-F granites. High evolved granites with Li-F facies have been described from many rare metal provinces in the world (Kovalenko et al., 1971, Gerel, 1990; Raimbault et al., 1995; Antipin, 2001).

High F content (Table 2) up to 1.15% produces highly mobile magma, which can reach high level in the crust. Li-F granites always occur in the highest level of leucocratic granites and crop out in the upper part of pluton forming cupola or crop out in the inner contact of multiphase plutons. (Kovalenko et al., 1971; Ivanov et al., 1984; Gerel, 1990; Koval, 1998).

The presence of late stage F-rich fluid is also important for metasomatic processes. Li-F granites are followed by albitites and microclinites, greisens and quartz veins with mineralization. Geochemical characteristics show that granites from Janchivlan pluton are very close to A2 type (8B) and differ from S type by higher

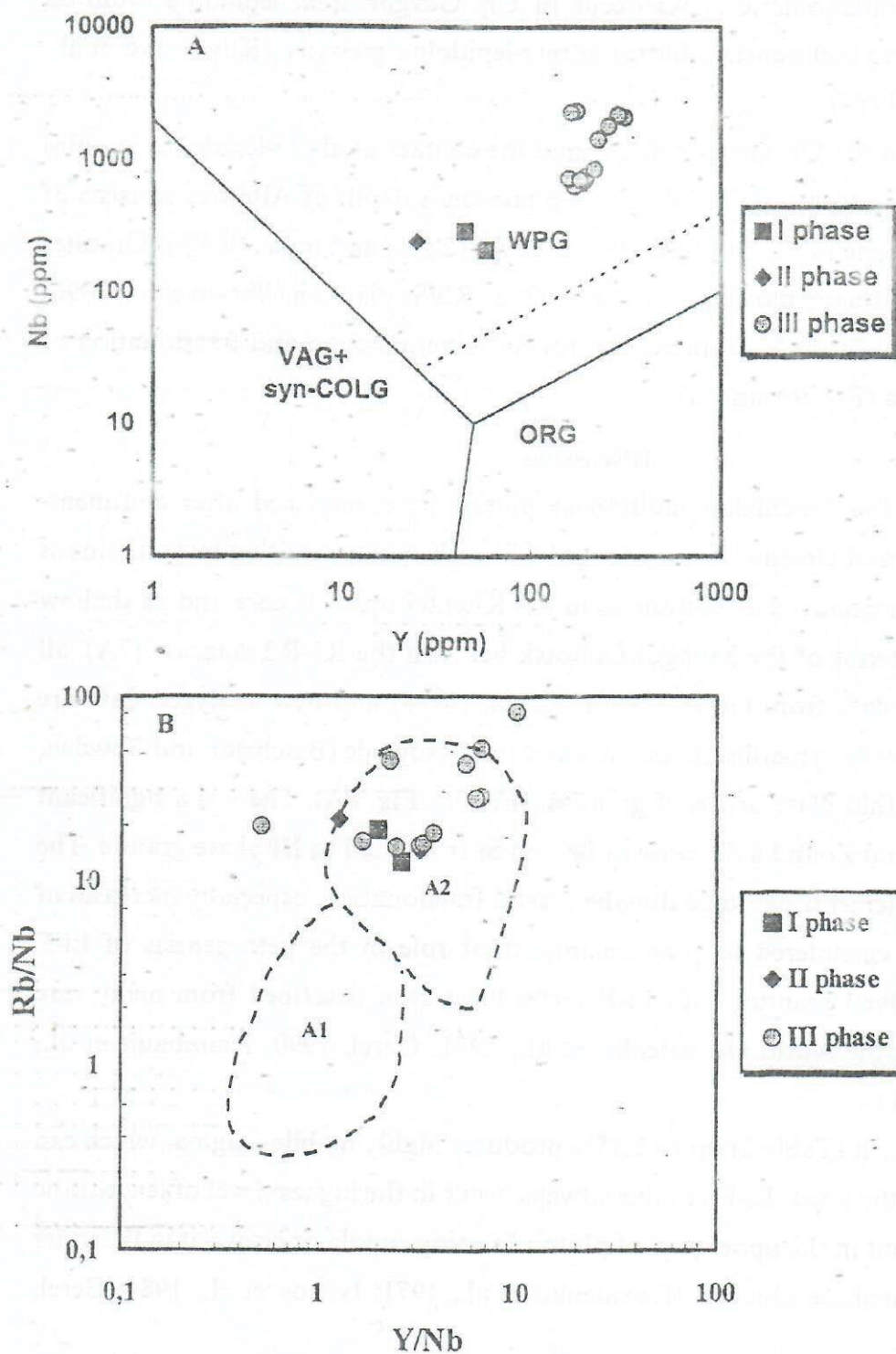


Fig.8. (A) Chemical compositions of granites from Janchivlan pluton on the Y versus Nb discrimination diagram of Pearce et al., (1984). (B) on the Rb/Nb versus Y/Nb diagram (Eby, 1990).

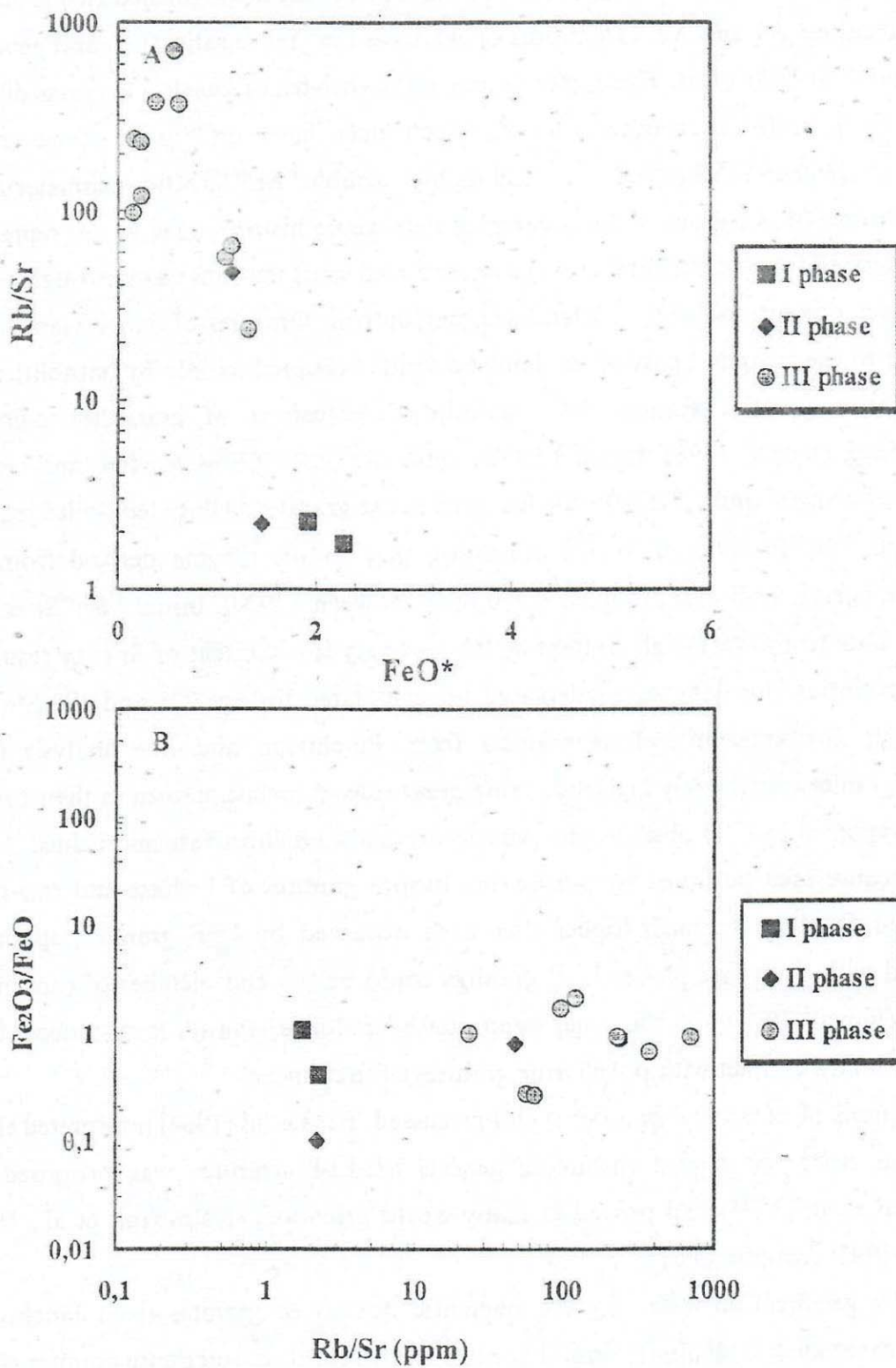


Fig. 9. Granites from Janchivlan pluton on the Rb/Sr versus. FeO* (A) Fe₂O₃/FeO versus Rb/Sr (B) diagrams. FeO* as (FeO+0.8998 Fe₂O₃).

alkalinity and abundance of Ta, Li, Be and Sn. Eby (1992) distinguished two groups of A type granites: A1 and A2. Granitoids of A1 have low Y/Nb ratio (1.2) and generally low initial $^{87}\text{Sr}/^{86}\text{Sr}$ ratio. These granites are differentiates of basaltic magmas directly derived from OIB-like mantle sources, which may have undergone some crustal interaction. Higher Y/Nb ratio (1.2-7) and highly variable $^{87}\text{Sr}/^{86}\text{Sr}$ ratios characterize A2 type. Granites of A2 group show a complex petrogenic history. This group represents magma derived from continental crust or underpleted crust that has been through a cycle continent-continent collision or island-arc magmatism. Granites of Janchivlan pluton emplaced in the marginal part of the Khentei uplift occupied mainly by batholiths and suggest have genetic relation with batholithic intrusions of granodiorite-granite composition. (Koval, 1998). Initial $^{87}\text{Sr}/^{86}\text{Sr}$ ratio is 0.7049-0.7044 for first and second phases accordingly, and 0.7187-0.7306 for third phase granites. Albite-lepidolite granites show high $^{87}\text{Sr}/^{86}\text{Sr}$ ratio of 0.7502 indicating that source magma derived from the continental crust. Li-F granites have Y/Nb ratio between 1.2-7.0. Initial $^{87}\text{Sr}/^{86}\text{Sr}$ is very variable. Due to the very high content of Rb and very low content of Sr they resulting age uncertainties Our data were calculated for calculated for age 225 and 190 Ma). Sr initial ratio for amazonite-albite granites from Janchivlan and one analysis from Avdrant granite is extremely high indicating great role of metasomatism in their origin. This is supported by field observation. Amazonite is always substitute microcline.

Because area occupied by porphyritic biotite granites of I phase and two-mica granites of II phase is much higher then area occupied by Li-F granites, spatially, associated with Two first phases Li-F granites could be the end member of rare metal granites. (Koval, 1998). On the other hand albite-lepidolite granites form independent body with sharp contact with porphyritic granites of first phase.

Genesis of rare metal granites is still discussed. Beus et al (1964) interpreted these granites as apogranites and magmatic genesis of Li-F granites was proposed by Kovalenko et al. (1971) and proved in many world provinces (Raimbault et al., 1995; Haapala, 1997; Antipin, 2001).

New geochemical data support magmatic genesis of granites from Janchivlan pluton and elevated K alkalinity, initial Sr ratio for first and second phase granites show a deep source involvement in origin of these granites. Granites of third phase are highly fractionated with complex magmatic and metasomatic signature. Because all analyzed

rocks are not plotted to one isochron we suggest metasomatism role in origin of amazonite-albite granites, and albitites.

References

1. Antipin V.S. (2001) Elvan-ongonite magmatism from various rare metal provinces. *Geology*, 4, 70-78.
2. Batchelor R.A. and Bowden P. (1985). Petrogenic interpretation of granitoid rock series using multicationic parameters. *Chemical Geology*, 48, 43-55.
3. Batjargal Sh., Gerel O, Baljinnyam et al. (1982). Geology and mineralogy of Elsetuin sulfide-cassiterite mineralization. *Mineralogical Museum Transactions*. 43-50. (in Russian)
4. Beus A.A., Severov E.A., Sitnin A.A. and Saubotkin K.D. (1962) Albitized and greisenized granites (apogranites). *Moskwa. Akademia Nauk SSSR*, pp.1- 196 (in Russian).
5. Blewett P.L., Chappel B.W. and Allen C.M. (1995), Intrusive metallogenic provinces in eastern Australia based on granite source and composition. *Origin of granites and related rocks* (ed. M. Brown, P.A. Candela, D.L. Peck, W.E. Stephens, R.J. Walker and E-an Zen). Royal Society of Edinburgh, 281-291
6. Chappel B.W. and White A.J.R. (1974). Two contrasting granite types. *Pacific Geology*. Vol. 8, 173-174.
7. Eby G.N. (1992). Chemical subdivision of the A-type granitoids: Petrogenetic and tectonic implications. *Geology*, v. 20, 641-644. *Geology of Mongolia*. (1973). (ed. Khasin R.A. and Marinov). M. Nedra. Volume II, pp.1-751 (in Russian).
8. Gerel O. (1978) Petrology and Geochemistry of granites with miarolitic pegmatites. PhD thesis. Irkutsk, pp.1-240 (in Russian).
9. Gerel O and Baljinnyam V. (1986) Petrology and mineralization of Janchivlan pluton. *Scientific notes*, 3. 15-25 (in Mongolian).
10. Gerel O. (1990). Petrology, geochemistry and mineralization of Mesozoic subalkaline granitoids in Mongolia. Irkutsk. Dr Sc Thesis. pp. 1-400 (in Russian)
11. Gerel O, Kanisawa S and Ishikawa K. (1999). Petrological characteristics of Granites from the Avdant and Janchivlan plutons, Khentii range, Central Mongolia. *Problems of Geodynamics and Metallogeny of Mongolia*. Transactions. Vol. 13, 34-39.
12. Haapala I. (1997). Magmatic and postmagmatic processes in tin-mineralized granites: topaz-bearing leucogranite in Eurajoki Rapakivi granite Stock, Finland. *Journal of Petrology*, v.38, No.12, 1645- 1659.
13. Iizumi, S. (1996). Sr and Nd analyses, using a thermal ionization mass spectrometer. MAT 262. *Geoscience Rept. Shimane Univ.*, 15, 153-159.
14. Komarov Yu.V., Belogolovkin A.A., Kopylov, E.N and Chuluun D. (1984) Structure and emplacement of Janchivlan massif. *Janchivlan rare metal granitic pluton, Central Mongolia*. Irkutsk. ISU printing house. 16-31 (in Russian)
15. Koval P. V. (1998). Regional geochemical analysis of granitoids. Novosibirsk Siberian branch RAS SPC UIGGM, pp. 1-492 (in Russian).
16. Kovalenko V.I., Kuzmin M.I., Zonenshain L.P. et al. (1971). Rare metal granitoids of Mongolia. M.: Nauka, pp.1-239 (in Russian).
17. Kovalenko V.I., Kuzmin M. I. (1974). Metasomatic zwitter and associated rare metal mineralization. (on example of ore deposits from Czechoslovakia and Mongolia) *Metasomatism and mineralization*, M Nauka, pp.1-364. (in Russian).
18. Kovalenko V.I. (1977). Petrology and geochemistry of rare metal granitoids. Nauka, pp. 1-206 (in Russian).
19. Kovalenko V. I., Yamolyuk V.V. and Bogatkov O. A. (1995). Magmatism, geodynamics and metallogeny of Central Asia. MIKO, pp.1-272.
20. Kovalenko V.I. and Kovalenko N.I. (1976). Ongonites (topaz bearing quartz keratophyres) subvolcanic analogous of lithium-fluorine granites. M. Nauka, pp. 1-127 (in Russian).
21. Lapidus I.L., Kovalenko V.I. and Koval P.V. (1977) Mica from rare metal granitoids. Novosibirsk: Nauka, pp. 1-104 (in Russian).

22. Le Maitre R.W., Bateman P., Dudek A. et al. (ed.). (1989) A classification of igneous rocks and glossary of terms: recommendation of the IUGS Subcommission on the Systematics of Igneous rocks. Oxford: Blackwell, pp. 1-193.
23. Luth W.C., Jahns R.N. and Tuttle O.F. (1964) The granite system at pressures of 4 to 10 kilobars. *J. Geophys. Res.* 69, 753-759.
24. Ivanov A.N., Rapatskaya L.A., Gerel O., Baljinnyam V. (1984) Granite Mineralogy and chemistry. Janchivlan rare metal granitic pluton, Central Mongolia. Irkutsk. ISU Printing house. 53-81 (in Russian)
25. Nagibina M. S. (1967). Tectonic structures related to activation and revivation. *Geotectonika*. 4. 15-26. (in Russian).
26. Novoselov S.V., Dugaraa P and Vakhromeev G.S. (1984) Deep structure of Janchivlan pluton Janchivlan rare metal granitic pluton, Central Mongolia. Irkutsk. ISU Printing house. 6-16 (in Russian)
27. Pearce J.A., Harris N.B.W., and Tindle, A.G. 1984. Trace element discrimination diagrams for the tectonic interpretation of granitic rocks *Journal of petrology*, v. 25, p. 956-983.
28. Pecerrillo A and Taylor S.R. Geochemistry of Eocene calc-alkaline volcanic rocks from the Kastamonu area, northern Turkey. *Contrib. Mineral. Petrol.* 58, 63-81
29. Pitcher W.S. 1983. Granite: topology, geological environment and melting relationship. In M.P. Atherton and C.D. Gribble, eds. *Migmatites, Melting and Metamorphism* Nantwich: Shiva, 277-287.
30. Rimbault L., Cuney M., Azencott C., Duthou L.L. and Joron J.L. (1995) Geochemical Evidence for a Multistage Magmatic Genesis of Ta-Sn-Li Mineralization in the Granite at Beauvoir, French Massif Central. *Economic Geology*, 90. 548-576.
31. Sizykh V.I., Dandar S., Dashdavaa S. and Sereegotov Ch. (1984) Janchivlan rare metal granitic pluton, Central Mongolia. Irkutsk. ISU Printing house, 81-106. (in Russian) Tectonics of Mongolia. (1974). M.(ed. Yanshin A.L.) M. Nauka pp. 1-284 (in Russian).
32. Tischendorf G., Forster H.J. and Gottesmann B. (1997) On Li-bearing micas: estimating Li from electron microprobe analyses and an improved diagram for graphical representation. *Mineralogical Magazine*, 61, 809-834.
33. Tischendorf, G., Forster H.J. and Gottesmann B. (1999) The correlation between lithium and magnesium in trioctahedral micas: Improved equations for Li₂O estimation from MgO data. *Mineralogical Magazine*, 63, 57-74.
34. Sheglov A.D. (1968) Metallogeny of autonomic activation regions. M. Nedra, pp. 1-180.
35. Whalen L.B., Currie K.L and Chappel B.W. (1987) A-type granites: Geochemical characteristics, discrimination and petrogenesis. *Contrib. Mineral. Petrol.* 95, 407-419.
36. Zonenshain L.P., Kuzmin M.I., Natapov L.M. (1990) Tectonics of lithosphere plates of the territory of USSR. M. Nedra, pp. (in Russian)